The Korean Journal of Ceramics, **5** [2] 99 - 103 (1999)

Microstructural Evolution during High-Temperature Deformation of Coarse-Grained $BaTiO_3$

Eun Tae Park*

Energy Technology Division, Argonne National Laboratory, Argonne, IL 60439, USA
(Received December 11, 1998)

Compressive creep of dense polycrystalline $BaTiO_3$, with average grain sizes of 19.3-52.4 μm, has been investigated at 1100-1300°C in air or under controlled atmospheres (10^2-10^5Pa O_2). Some cavity growth occurred during deformation because of non-steady-state damage accumulation in the form of cavitation. Comparison of the creep data of polycrystalline $BaTiO_3$ with existing diffusivity and creep data for perovskite oxides suggested that deformation of polycrystalline $BaTiO_3$ was controlled by the extrinsic lattice diffusion of barium or titanium.

Key words : Creep, $BaTiO_3$, diffusion

I. Introduction

The perovskite oxide $BaTiO_3$ is a ferroelectric compound whose electrical properties have been studied extensively because of the oxide's many technical applications, including sensors, transducers, and actuators.[1] The technological importance of $BaTiO_3$ has been demonstrated repeatedly, and its physical properties in ceramic form have been thoroughly investigated. Many studies have also focused on point defects, diffusion, and electrical conductivity of $BaTiO_3$.[2-8]

Despite the importance of this information to processing and ultimate component performance of $BaTiO_3$, few investigations have focused on high-temperature mechanical behavior of these materials.[9-11] High-temperature deformation mechanisms most commonly observed in ceramics are controlled by diffusion of the slowest-moving species. In addition, when high-temperature deformation, creep, is controlled by diffusion, study of creep rate as a function of temperature is an alternative way to measure the diffusion coefficient of the rate-controlling species.

Recently, we investigated compressive creep of dense $BaTiO_3$ having linear-intercept grain sizes of 19.3-52.4 μm at 1200-1300°C by varying the oxygen partial pressure from 10^2 to 10^5 Pa in both constant-stress and constant-crosshead-velocity methods.[11] The stress exponent was ≈ 1, the grain-size dependence was $\approx 1/d^2$, and the activation energy was ≈ 720 kJ/mole. These parameters, combined with the microstructural observation (particularly grain displacement and absence of deformation-induced dislocations) indicated that the dominant deformation mechanism was grain-boundary sliding accommodated by lattice cation diffusion.

*Now with Dept. of Mater. Sci. & Engr., U of Cincinnati, Cincinnati, OH, USA

The purpose of this study is to further investigate the microstructural evolution during high-temperature creep of coarse-grained $BaTiO_3$ materials by scanning electron microscopy (SEM) and transmission electron microscopy (TEM). Also, creep data are compared with existing diffusion data to identify rate-controlling species in $BaTiO_3$. The information gathered in this paper will add to the body of knowledge on this useful and scientifically interesting technical material.

II. Experimental Procedure

Preparation of our high-density polycrystalline $BaTiO_3$ specimens has been described.[11] To obtain microstructures of various grain sizes, specimens were sintered at 1320°C for 0.5 h, 1320°C for 2 h and 1360°C for 2 h in flowing O_2 or air with a heating rate of 200°C/h and a cooling rate of 60°C/h. The average linear-intercept grain sizes were 19.3±1.6, 30.9±2.0 and 52.4±4.0 μm for the specimens sintered at 1320°C for 0.5 h, 1320°C for 2 h and 1360°C for 2 h, respectively. The densities of all specimens were higher than 97% of theoretical density.

Three different-grain-sized $BaTiO_3$ specimens ($\approx 3 \times 3 \times 6$ mm) were deformed in compression between Al_2O_3 platens in air or a controlled P_{O_2} atmosphere ($10^2 < P_{O_2} < 10^5$ Pa) in one of the two following ways at 1100-1300°C: (i) at constant crosshead velocity; or (ii) at constant stress.

The microstructures of the as-sintered and deformed $BaTiO_3$ specimens were characterized by X-ray diffraction (XRD), density measurements, SEM, and TEM. XRD patterns for polycrystalline $BaTiO_3$ specimens revealed only $BaTiO_3$ peaks, and there was no difference between the samples with different sintering conditions. For TEM, samples were polished, dimpled, and then ion-milled to produce electron-transparent foils.

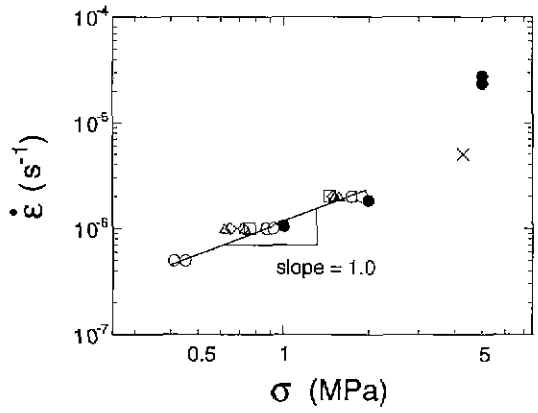

Fig. 1. Log-log plot of strain rate versus stress for 30.9 μm grain-sized specimens deformed at 1300°C in air (closed circles) or under controlled P_{O_2} (open circles=10^5, diamonds=10^4, squares=10^3, and triangles=10^2 Pa); X=fractured.

III. Results and Discussion

Fig. 1 presents results of an experiment performed on the 30.9 μm grain-sized specimen at 1300°C in controlled P_{O_2} atmospheres (10^2-10^5 Pa) at constant crosshead velocity ($\varepsilon=5\times10^{-7}$ to 5×10^{-6} s^{-1}) and in air ($P_{O_2}=2\times10^4$ Pa) under constant stress (σ=1, 2, and 5 MPa) in order to determine the stress exponent. For tests at constant crosshead velocity, the sample was fractured at 4.29 MPa with strain rate of 5×10^{-6} s^{-1}, which is indicated by the X in the figure. The stress exponent for the $BaTiO_3$ tested in O_2 was 1.0 ± 0.2 at the strain rates between 5×10^{-7} and 2×10^{-6} s^{-1}. There was excellent agreement between constant-stress and constant-crosshead-velocity tests at strain rate of 2×10^{-6} s^{-1}. The stress exponent tested in air became >1 at higher stress.

The average stress exponent is 1.0 ± 0.2 and grain size exponent is 1.8 ± 0.3, which indicates that the creep mechanism of $BaTiO_3$ occurs via lattice diffusion.[11] Some diffusional creep models predict existence of a threshold stress (σ_0).[12] The threshold stress is the minimum stress at which a material can be plastically deformed and is related to strain rate, $\varepsilon\propto(\sigma-\sigma_0)$, in creep tests. To calculate the threshold stress, a linear plot of stress versus strain rate for three-grain sized samples was constructed (Fig. 2). The results of Fig. 2 reveal a threshold stress $\approx0\pm0.2$ MPa independent of grain sizes, implying that there is

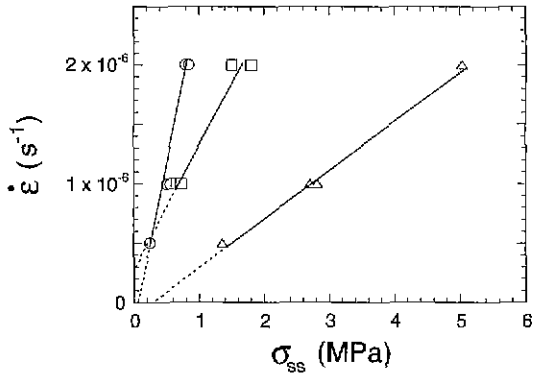

Fig. 2. Linear plot of strain rate versus steady-state stress for $BaTiO_3$ specimens deformed at 1300°C in $P_{O_2}=10^4$ Pa with different grain sizes. Circles represent 19.3 μm, squares 30.9 μm, and triangles 52.4 μm grain-sized specimen.

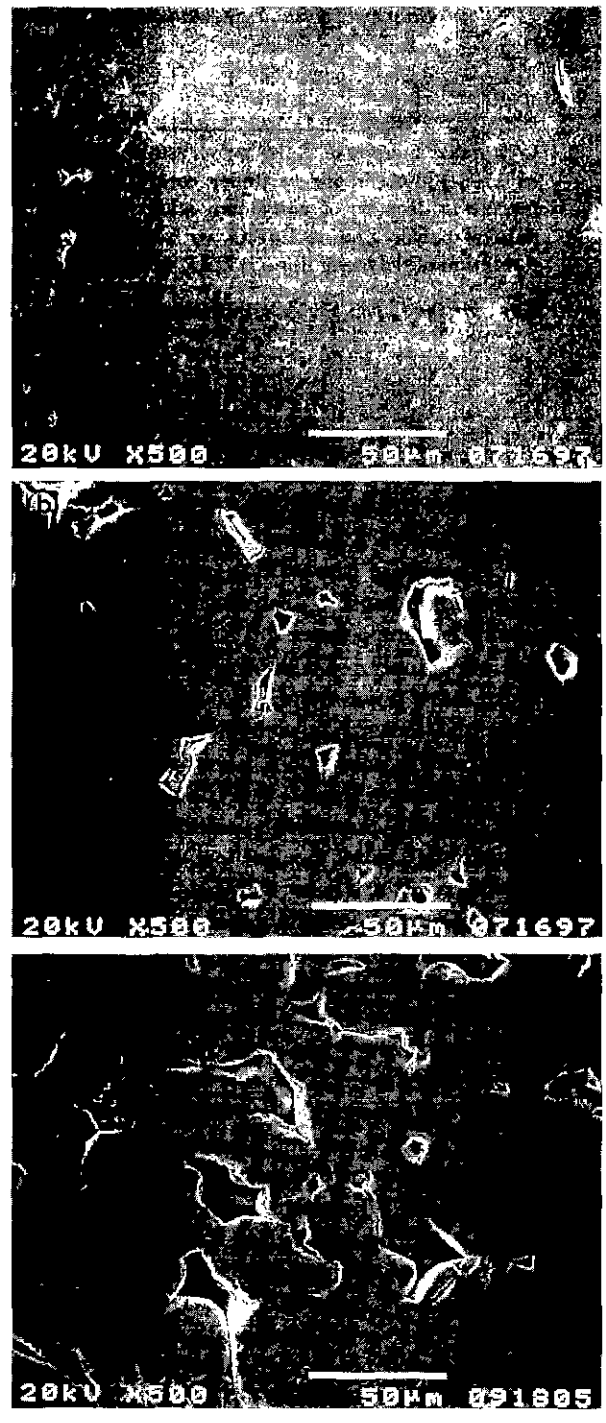

Fig. 3. SEM photomicrographs of pore sizes and shapes before and after deformation: (a) sintered 30.9 μm grain-sized sample, (b) deformed $\approx1.5\%$ at 1300°C in O_2 at $\dot{\varepsilon}=1\times10^{-6}$ and 2×10^{-6} s^{-1} and (c) deformed $\approx1.4\%$ at 1300°C in O_2 at $\dot{\varepsilon}=1\times10^{-6}$, 2×10^{-6} and 5×10^{-6} s^{-1}.

no threshold stress.

SEM micrographs of pore sizes and shapes within a specimen before and after deformation are shown in Fig. 3. The microstructure of the sintered specimen (Fig. 3(a)) contains a mixture of small cavities (1-3 μm) and a few larger triple-point pores (8-12 μm). However, in the specimen deformed at 1300°C in O_2 at $\varepsilon=1\times10^{-6}$ and 2×10^{-6} s^{-1} (Fig. 3b)), for which the maximum steady-state stress was 1.74 MPa, several pores grew significantly. In the sample deformed at three strain rates, including a high strain rate of 5×10^{-6} s^{-1} (Fig. 3 (c)), steady state was achieved at the strain rates of 1×10^{-6} and 2×10^{-6} s^{-1}; however, the sample fractured at a strain rate of 5×10^{-6} s^{-1}, at which the maximum stress was 4.29 MPa. The microstructure of this sample was quite different from that observed in the sample deformed at only lower strain rates of 1×10^{-6} and 2×10^{-6} s^{-1} (Fig. 3(b)). The cavity density greatly increased and the cavities grew. It can be seen that the material developed extensive cavitation during deformation, with cavity size being similar or larger than the average grain size ($\approx$31 μm).

The TEM study focused on dislocation activity and cavity formation in the deformed samples. A TEM photomicrograph of an undeformed 30.9 μm grain-sized specimen is shown in Fig. 4. Such stepped, low-angle grain boundaries were commonly observed. No significant dislocation activity was observed. Fig. 5 shows a dark-field TEM image of a specimen deformed $\approx$1% at 1300°C in O_2 at constant crosshead velocity of 5×10^{-7} and 1×10^{-6} s^{-1} for which steady state was achieved. A crack which resulted from deformation is clearly visible. The arrow in the micrograph indicates debris probably from specimen preparation. For observation of dislocations in deformed samples, bright-and dark-field images were investigated with $g_{<101>}$ and $g_{<001>}$; however, few dislocations were observed in the grains. The grain boundaries of the deformed specimen were clean, and no second phases were observed.

In the microstructure of the deformed sample shown in Fig. 3(b) and (c), growth of cavities increased with increasing stress to accommodate deformation by grain-boundary sliding. The growth and coalescence of cavities are due to the diffusion of vacancies out of the boundary to the surface of voids subjected to a tensile stress.[13] Although the cavities in the deformed $BaTiO_3$ were similar in appearance to those observed in the Y_2O_3-stabilized ZrO_2 polycrystals by Bravo-Len *et al.*,[14] the creep results between the two studies differed with respect to existence of a threshold stress. Cavitation in both cases is a result of grain-boundary sliding not fully accommodated by diffusion.

The increase of cavity density and size at 4.29 MPa (Fig. 3(c)) is probably due to stress concentration at triple points causing preexisting cavities to grow during deformation. Therefore, the micrographs in Fig. 3(b) and (c) provide additional support for grain-boundary sliding,

Fig. 4. TEM micrograph of undeformed 30.9 μm grain-sized $BaTiO_3$ specimen.

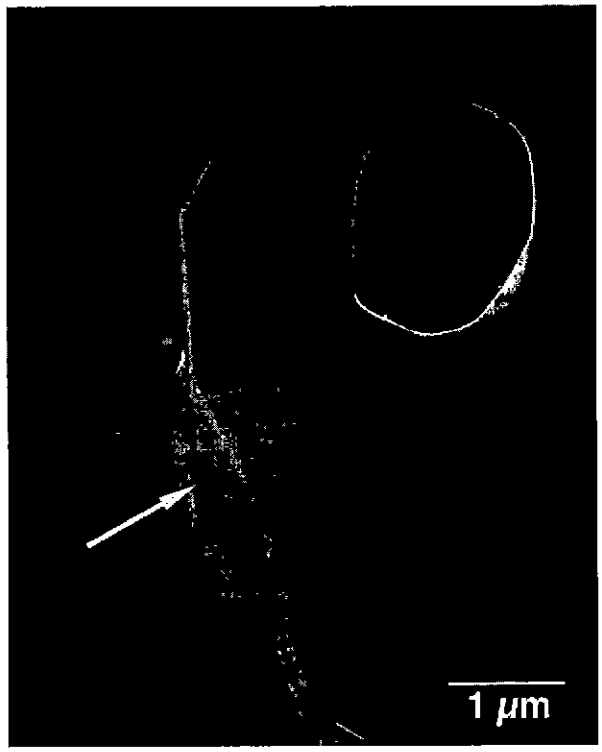

Fig. 5. Dark-field TEM image of damage in the 30.9 μm grain-sized sample deformed $\approx$1% at 1300°C in O_2.

which was only partially accommodated by diffusion.

According to the creep data and microstructures of the deformed samples, it is concluded that the deformation of $BaTiO_3$ was only a quasi-steady-state. This assertion is based on the reproducibility of stress (or strain rate) which was very good, but recognizing that non-steady-state phenomena of damage accumulation in the form of cavitation was observed. The cavitation resulted in values of n>1. The crack shown in TEM micrograph (Fig. 5) resulted from damage accumulation during creep supports cavitation phenomena. Therefore, the total strain, ε_T, of the deformed $BaTiO_3$ sample can be expressed by the following equation:

$$\varepsilon_T=\varepsilon_P+\varepsilon_D \quad (1)$$

where ε_P and ε_D are the strain occurring by the plasticity and damage, respectively.

For specimens crept in the n=1 region, the reproducibility of the σ versus ε data, and the fact that the σ versus $\dot{\varepsilon}$ curve (Fig. 1) does not depend on the sequence of stress changes (i.e., is path independent), indicates that $\varepsilon_P>>\varepsilon_D$, and that the data can be described by a steady-state creep mechanism. However, as stress increases, ε_D becomes more important and a steady-state approximation is not valid. The stress exponent increases as the damage proceeds.

Fig. 6 shows a plot of the logarithm of lattice barium[15] and oxygen[16] diffusivity in $BaTiO_3$ versus the reciprocal of absolute temperature obtained from Eqs. 2 and 3, respectively.

$$D_{Ba}=0.8\exp\left(-\frac{372{,}000}{RT}\right)\text{cm}^2/\text{sec.} \quad (2)$$

$$D_O=3.7\times10^{-7}\exp\left(-\frac{47{,}700}{RT}\right)\text{cm}^2/\text{sec.} \quad (3)$$

For comparison, the Raj-Ashby model equation (Eq. 4)[17] was used to determine the diffusivity of the rate-controlling diffusing species of $BaTiO_3$ from the creep data:

$$\dot{\varepsilon}=\frac{B^*\sigma\Omega D_L}{kTd^2} \quad (4)$$

where B^* is a constant equal to 40, D_L the lattice diffusivity of rate-controlling species, k Boltzmann's constant, and T the temperature. In this equation, the atomic volume, Ω, was taken as the unit cell volume divided by the number of atoms in the unit cell (1.276×10^{-29} m^3 for $BaTiO_3$) and the spatial grain size, d, was calculated from $d=1.57\times GS$,[18] where GS is the average grain size measured by the intercept method. The D_L values were determined from Eq. 4 and steady-state creep data.

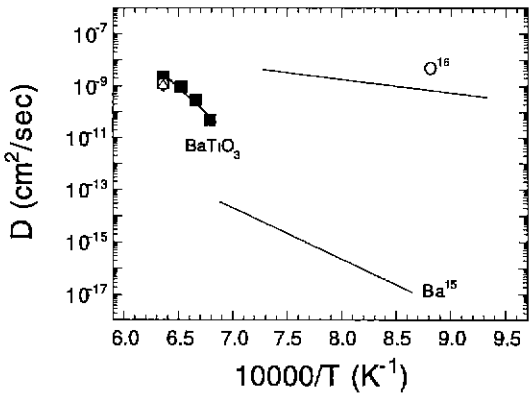

Fig. 6. Diffusivity versus reciprocal absolute temperature of $BaTiO_3$, barium,[15] and oxygen.[16] Open points indicate constant-crosshead velocities, closed points indicate constant stress. Squares represent 19.3 μm grain-sized specimen deformed in air, diamonds 30.9 μm in air, circles 30.9 μm in $P_{O_2}=10^5$ Pa, and triangles 52.4 μm in $P_{O_2}=10^4$ Pa.

The calculated values of $BaTiO_3$ creep data are also shown in Fig. 6. From the plot of diffusivity versus reciprocal absolute temperature, it is observed that the calculated diffusivity of the rate-controlling species of $BaTiO_3$ (D_{BaTiO_3}) is higher than barium diffusivity (D_{barium}), and lower than oxygen diffusivity (D_{oxygen}). The observation that D_{BaTiO_3} is lower than D_{oxygen} supports the conclusion that the lattice diffusion of the cations, rather than oxygen lattice diffusion, controls the deformation rate of $BaTiO_3$. However, D_{BaTiO_3} is ~10^3 higher at 1200°C and ~4×10^3 higher at 1300°C than D_{barium}, if D_{barium} is calculated from Eq. 4 and extrapolated to higher temperatures between 1200-1300°C.

It is difficult to compare data of D_{BaTiO_3} and D_{barium}. Verduch and Lindner[15] did not mention the purity of their $BaTiO_3$ specimens, and atmospheric conditions for measuring the self-diffusion of barium were not reported. The difference between D_{BaTiO_3} and D_{barium} is difficult to explain. It is highly possible that diffusion of Ti controls creep of $BaTiO_3$. However, Ti diffusion has not been measured in $BaTiO_3$.

IV. Conclusions

Polycrystalline $BaTiO_3$ specimens of various linear-intercept grain sizes (19.3-52.4 μm) were deformed at 1100-1300°C in air or under controlled P_{O_2} atmosphere (10^2-10^5 Pa) at constant crosshead velocity $\dot{\varepsilon}=5\times10^{-7}$-$5\times10^{-6}$ s^{-1}) or constant stress (σ=1-5 MPa). The microstructural evolution during creep of coarse-grained $BaTiO_3$ shows quasi-steady state with some cavity formation and few dislocations activity. The creep data and microstructural observations indicated that creep of polycrystalline $BaTiO_3$ was controlled by lattice diffusion of barium or titanium.

Acknowledgments

The author is grateful to Russell Cook and Roseann Csencsits for their invaluable assistance with electron microscopy, and to Ken Goretta, Jeff Wolfenstine, An-

tonio R. De Arellano-López, and Jules Routbort for stimulating discussions. This work was supported by the U.S. Department of Energy, under Contract W-31-109-Eng-38.

References

1. F. Jona and G. Shirane, Ferroelectric Crystals, pp. 108-215, Dover, New York, 1993.
2. G. Arlt, "Twinning in Ferroelectric and Ferroelastic Ceramics: Stress Relief," *J. Mater. Sci.*, **25**, 2655-2666 (1990).
3. J. F. Baumard, P. Abelard, and J. Lecompte, "The Defect Structure of Donor-Doped $BaTiO_3$," *J. Phys. Colloque CI Suppl.*, **47**, 867-870 (1986).
4. N. H. Chan and D. M. Smyth, "Defect Chemistry of $BaTiO_3$," *J. Electrochem. Soc.*, **123**(10), 1584-1585 (1976).
5. N. H. Chan and D. M. Smyth, "Defect Chemistry of Donor-Doped $BaTiO_3$," *J. Am. Ceram. Soc.*, **67**(4), 285-288 (1984).
6. Z. Li, S.-K. Chan, M. H. Grimsditch, and E. S. Zouboulis, "The Elastic and Electromechanical Properties of Tetragonal $BaTiO_3$ Single Crystals," *J. Appl. Phys.*, **70**(12), 7327-7332 (1991).
7. S. A. Long, and R. N. Blumenthal, "Ti-Rich Nonstoichiometric $BaTiO_3$: I. High-Temperature Electrical Conductivity Measurements," *J. Am. Ceram. Soc.*, **54**(10), 515-519 (1971).
8. A. M. J. M. Seuter, "Defect Chemistry and Electrical Transport Properties of Barium Titanate," *Philips Res. Rep. Suppl.*, **3**, 1-84 (1974).
9. S. Beauchesne and J. P. Poirier, "Creep of Barium Titanate Perovskite: A Contribution to a Systematic Approach to the Viscosity of the Lower Mantle," *Phys. Earth Planet. Inter.*, **55**, 187-199 (1989).
10. C. Carry and A. Mocellin, "Superplastic Creep of Fine-Grained $BaTiO_3$ in a Reducing Environment," *J. Am. Ceram. Soc.*, **69**(9), C-215-C-216 (1986).
11. E. T. Park, P. Nash, J. Wofenstine, K. C. Goretta, and J. L. Routbort, "High-Temperature Deformation of Polycrystalline $BaTiO_3$," *J. Mater. Res.*, **14**(2), 523-528 (1999).
12. M. F. Ashby and R. A. Verrall. "Diffusion-Accommodated Flow and Superplasticity," *Acta Metall.*, **21**(2), 149-163 (1973).
13. J. Philibert, Atom Movements; Diffusion and Mass Transport in Solids, pp. 421-520, Les Editions de Physique, France, 1991.
14. A. Bravo-León, M. Jimónez-Melendo, and A. Domínguez-Rodriguez, "High Temperature Plastic Deformation at Very Low Stresses of Fine-Grained Y_2O_3-Partially Stabilized ZrO_2," *Scripta Mater.*, **35**(4), 551-555 (1996).
15. A. G. Verduch and R. Lindner, "Self-Diffusion in Barium Metatitanate," *Arkiv. Kemi.*, **5**(29), 313-316 (1953).
16. J. Doskocil and Z. Pospisil, "Measurement of Oxygen Self-Diffusion Coefficient in Some Titanate Ceramics," *Silikaty*, **2**, 113-121 (1972).
17. R. Raj and M. F. Ashby, "On Grain Boundary Sliding and Diffusional Creep," *Metall. Trans.*, **2**(4), 1113-1127 (1971).
18. E. E. Underwood, "Quantitative Metallography, pp. 123-134 in Metals Handbook Ninth Edition, Vol. 9, Metallography and Microstructures," Ed. by ASM Handbook Committee, American Society for Metals, Metals Park, OH, 1985.